INTERNATIONAL JOURNAL FOR NUMERICAL METHODS IN FLUIDS
Int. J. Numer. Meth. Fluids 2004; **44**:1355–1376 (DOI: 10.1002/fld.695)

Analysis of hypersonic flows using finite elements with Taylor–Galerkin scheme

Martin P. Kessler[1] and Armando M. Awruch[2,*,†]

[1] *PROMEC, Universidade Federal do Rio Grande do Sul, Brazil*
[2] *PPGEC, Universidade Federal do Rio Grande do Sul, Av. Osvaldo Aranha, 99, 3 andar, Porto Alegre 90035-190, RS, Brazil*

SUMMARY

The aim of the present work is to introduce a formulation for the numerical analysis of three-dimensional thermochemical non-equilibrium hypersonic flows, using the finite element method and the Taylor–Galerkin scheme and adopting Park's 2-temperature, 5-species (N_2, O_2, NO, N and O) and 17-reaction model. Examples using Euler and Navier–Stokes equations are included and compared with experimental and numerical works presented by other authors. The results are close to those analysed by other researches and a good computational performance was obtained. Copyright © 2004 John Wiley & Sons, Ltd.

KEY WORDS: hypersonic flow; thermochemical non-equilibrium; numerical simulation; finite elements

1. INTRODUCTION

Reentering the Earth's atmosphere is a phenomenon that has challenged researchers over the last few decades. Owing to the growth of space exploration and the increasing number of space trips, great interest in dominating launch, orbit and recovery of space vehicles has been created, primarily to bring back people and experiments safely to Earth.

Since the beginning of the Space Age, marked by the Sputnik launch in 4th October 1957, great interest in operating recoverable space vehicles is being created by researchers and scientists. The recovery of a space vehicle is a very complex procedure, including its reentry into the Earth's atmosphere at large speeds, usually reaching the hypersonic regime (Mach > 5). For an orbital vehicle, reentry starts at Mach $= 25$ approximately (around 8 km/s),

*Correspondence to: A. M. Awruch, PPGEC, Universidade Federal do Rio Grande do Sul, Av. Osvaldo Aranha, 99, 3 andar, 90035-190 Porto Alegre, RS, Brazil.
†E-mail: awruch@adufrgs.ufrgs.br

Contract/grant sponsor: National Supercomputing Center of the Federal University of Rio Grande de Sul
Contract/grant sponsor: Brazilian Space Agency

Received 7 May 2003
Revised 10 December 2003

and for a vehicle returning from the Moon, as performed by Apollo, reentry starts at Mach = 36 approximately (around 11 km/s). Owing to these high speeds, extremely high temperatures are generated around the vehicle, which may cause vibrational excitation, dissociation and ionization of the molecules. Therefore, the perfect gas hypothesis is no longer valid for air at those regimes and one must include high temperature effects in the mathematical model to properly analyse hypersonic flows.

For high temperature analysis, knowledge of thermodynamic gas properties is needed. Some of those properties cannot be obtained from classic thermodynamics. On the other hand, statistic thermodynamics allows scientists to obtain those properties from basic principles. For a simple diatomic molecule ('dumbbell' model), the internal energy can be split into four modes: translational, rotational, vibrational and electronic [1]. Above specific temperatures (around 800 K for air at 1 atm), the molecules become vibrationally excited and the energy modes could be represented by more than one single temperature (thermal non-equilibrium).

For high-temperature hypersonic flows with chemical reactions, the vibrational temperature is very important, because it controls the molecular dissociation rate [2]. Park [3] suggests that without taking into account the vibrational temperature, there is a little chance that a CFD analysis be able to reproduce the experimentally observed phenomena. Lee [4] presented a basic formulation for flight analysis of aeroassisted orbital transfer vehicles (AOTV), which includes three energy conservation equations: total, vibrational and electronic. Park [5] introduced a simpler version, with only two energy conservation equations (total and vibrational), where vibrational and electronic temperature, T_v, are considered to be in equilibrium, but independent of the translational-rotational temperature, T.

Supersonic flow around a blunt body were first solved numerically by Moretti and Abbett [6]. They employed a time-marching finite difference technique, developed by Lax and Wendroff [7–9], applied to the transient Euler equations. Computer codes including physical phenomena present in hypersonic flows appeared in the early 1970s [10]. In the context of the finite element method (FEM), Donea [11] developed a time-marching procedure, the Taylor–Galerkin scheme, which is considered the equivalent of Lax–Wendroff method for FEM [12, 13]. Argyris *et al.* [14–17] applied the Taylor–Galerkin scheme to analyse the reentry of the European space vehicle, Hermes, into the Earth's atmosphere. They used a hypersonic mathematical model with chemical reactions and thermal equilibrium (one temperature).

The aim of the present work is to introduce a procedure to solve thermochemical non-equilibrium hypersonic flows using the Taylor–Galerkin scheme and Park's two-temperature model. Ionization is neglected, and only five chemical species are considered (N_2, O_2, NO, N and O). Three examples are presented: the hypersonic flow of partially dissociated nitrogen over a cylinder, the hypersonic flow over an half-ellipse and the diffusive hypersonic flow over an half-sphere.

2. THE MATHEMATICAL MODEL

2.1. Governing equations

A formulation for non-diffusive thermochemical non-equilibrium hypersonic flows is presented. Einstein notation is used, so summation along repeated indexes occur unless otherwise indicated. Subscript s refers to the species. Five different types of conservation equations are

applied: mass of the mixture, mass for each species, momentum, vibrational and total energies. They are gathered in a compact form, as follows:

$$\frac{\partial U}{\partial t}+\frac{\partial F_j}{\partial x_j}+\frac{\partial G_j}{\partial x_j}+H=0 \quad \text{in } \Omega \tag{1}$$

where

$$U=\begin{Bmatrix}\rho\\ \rho_s\\ \rho u_i\\ \rho e_{\mathrm{v}}\\ \rho e\end{Bmatrix},\quad F_j=\begin{Bmatrix}\rho u_j\\ \rho_s u_j\\ \rho u_i u_j+p\delta_{ij}\\ \rho e_{\mathrm{v}} u_j\\ (\rho e+p)u_j\end{Bmatrix},\quad G_j=\begin{Bmatrix}0\\ -J_{s,j}\\ -\tau_{ji}\\ -q_{\mathrm{v},j}-h_{\mathrm{v},s}J_{s,j}\\ -q_j-h_s J_{s,j}-u_j\sum_{k=1}^{3}\tau_{jk}\end{Bmatrix}$$
$$H=\begin{Bmatrix}0\\ -\omega_s\\ 0\\ -\omega_{\mathrm{v}}\\ 0\end{Bmatrix} \tag{2}$$

where ρ is the specific mass of the mixture, ρ_s is the specific mass of the species s, u_i is the velocity component in x_i direction, δ_{ij} is the Kronecker delta, $h_{\mathrm{v},s}$ and h_s are the vibrational and total enthalpy of species s, respectively, $J_{s,\mathrm{j}}$ is the mass flux vector, τ_{ij} is the stress tensor, $q_{\mathrm{v},j}$ and q_j are the vibrational and total heat flux vectors, respectively, ω_s and ω_{v} are the mass and vibrational/electronic energy sources, respectively, and Ω is the domain. The pressure p is obtained from Dalton's law of partial pressures, as follows:

$$p=\sum_{s=1}^{N_s}p_s=\sum_{s=1}^{N_s}\rho_s R_s T \tag{3}$$

where p_s and R_s are the partial pressure and the gas constant for species s, respectively, T is the translational temperature and N_s is the number of species. The vibrational energy, e_{v}, and the total energy, e, are defined by

$$\begin{aligned} e_{\mathrm{v}}&=c_s e_{\mathrm{v},s}\\ e&=\tfrac{1}{2}u_j u_j+c_s(e_{\mathrm{t},s}+e_{\mathrm{v},s}+e_{0,s})\end{aligned} \tag{4}$$

with

$$e_{\mathrm{t},s}=\begin{cases}\frac{3}{2}R_s T, & s=\text{atom}\\ \frac{5}{2}R_s T, & s=\text{molecule}\end{cases} \tag{5}$$

Table I. Data for the five species.

	N_2	O_2	NO	N	O
M_s (kg/kg mol)	28.02	32.00	30.01	14.01	16.00
R_s (J/kg K)	296.7	259.8	277.04	593.6	519.6
$e_{0,s}$ (J/kg)	0	0	2.99×10^6	33.59×10^6	15.42×10^6
$\theta_{v,s}$ (K)	3393	2270	2740	—	—
$\theta_{e,s}$ (K)	—	11390	174	—	228
G_s	0	0.6667	1	0	0.6
σ_s (Å)	3.798	3.467	3.492	3.298	3.050
$T_{\varepsilon,s}$ (K)	71.4	106.7	116.7	71.4	106.7

$$e_{v,s} = \begin{cases} 0, & s = \text{atom} \\ \dfrac{R_s \theta_{v,s}}{\exp(\theta_{v,s}/T_v) - 1}, & s = \text{molecule} \end{cases} \tag{6}$$

where c_s is the mass fraction, T_v is the vibrational temperature, $e_{t,s}$ and $e_{v,s}$ are the translational and vibrational internal energies, respectively, $e_{0,s}$ is the formation energy and $\theta_{v,s}$ is the vibrational characteristic temperature. The data for each of the five species are given in Table I.

Boundary conditions must be applied to velocities components u_i, specific mass of the mixture ρ, specific mass of the species s, ρ_s, translational temperature, T, and vibrational temperature, T_v, in the parts Γ_u, Γ_ρ, Γ_{ρ_s}, Γ_T and Γ_{T_v}, respectively, of the total boundary Γ. Initial conditions must also be given for the unknown variables in the domain Ω.

2.2. Diffusion coefficients

The diffusion coefficients are given by

$$J_{s,j} = \rho D_s \frac{\partial y_s}{\partial x_j} \quad \text{(no summation on } s\text{)} \tag{7}$$

$$\tau_{ij} = \mu \left(\frac{\partial u_i}{\partial x_j} + \frac{\partial u_j}{\partial x_i} \right) + \lambda \frac{\partial u_k}{\partial x_k} \delta_{ij} \tag{8}$$

$$q_{v,j} = \eta_v \frac{\partial T_v}{\partial x_j}, \quad q_j = \eta \frac{\partial T}{\partial x_j} + \eta_v \frac{\partial T_v}{\partial x_j} \tag{9}$$

where y_s is the mole fraction of species s, D_s is the effective diffusion coefficient for species s, μ is the mixture viscosity, λ is the volumetric viscosity ($\lambda = -2\mu/3$ when Stokes' hypothesis is assumed), T and T_v are the translational and the vibrational temperatures, respectively, η_v and η are the vibrational and total thermal conductivity coefficients, respectively. These coefficients are given by statistic thermodynamics, as follows [18]:

$$D_s = \frac{\gamma_{tot}^2 M_s (1 - M_s \gamma_s)}{\sum_{\substack{r=1 \\ r \neq s}}^{N_s} (\gamma_s / D_{sr})} \quad \text{(no summation on } s\text{)} \tag{10}$$

$$D_{sr} = 1.8583 \times 10^{-7} \frac{\sqrt{T^3 \left(\frac{M_s + M_r}{M_s M_r}\right)}}{p \sigma_{sr}^2 \Omega_{sr}} \quad \text{(no summation on } s\text{)} \tag{11}$$

$$\mu = \frac{y_s \mu_s}{y_r \Phi_{sr}} \tag{12}$$

$$\mu_s = 2.6693 \times 10^6 \frac{\sqrt{M_s T}}{\sigma_s^2 \Omega_s} \tag{13}$$

$$\eta = \eta_{\mathrm{t}} + \eta_{\mathrm{v}} \tag{14}$$

$$\eta_{\mathrm{v}} = k \sum_{\text{molec.}} \frac{\gamma_s}{\gamma_r \Delta_{sr}^{(1)}(T)} \tag{15}$$

$$\eta_{\mathrm{t}} = \frac{15}{4} k \frac{\gamma_s}{a_{sr} \gamma_r \Delta_{sr}^{(2)}(T)} \tag{16}$$

where

$$\Omega_{sr} \cong \left(\frac{T}{T_{sr}^*}\right)^{-0.145} + \left(\frac{T}{T_{sr}^*} + 0.5\right)^{-2.0} \tag{17}$$

$$\Omega_s \cong 1.147 \left(\frac{T}{T_{\varepsilon,s}}\right)^{-0.145} + \left(\frac{T}{T_{\varepsilon,s}} + 0.5\right)^{-2.0} \tag{18}$$

$$\Phi_{sr} = \frac{1}{\sqrt{8}} \left(1 + \frac{M_s}{M_r}\right)^{-1/2} \left[1 + \left(\frac{\mu_s}{\mu_r}\right)^{1/2} \left(\frac{M_r}{M_s}\right)^{1/4}\right]^2 \tag{19}$$

$$\Delta_{sr}^{(1)}(T) = \frac{8}{3} \left[\frac{2 M_s M_r}{\pi \bar{R} T (M_s + M_r)}\right]^{1/2} \pi \Omega_{sr} \quad \text{(no summation on } s \text{ or } r\text{)} \tag{20}$$

$$\Delta_{sr}^{(2)}(T) = \frac{16}{5} \left[\frac{2 M_s M_r}{\pi \bar{R} T (M_s + M_r)}\right]^{1/2} \pi \Omega_s \quad \text{(no summation on } s \text{ or } r\text{)} \tag{21}$$

$$a_{sr} = 1 + \frac{(1 - M_s/M_r)(0.45 - 2.54 M_s/M_s)}{(1 + M_s/M_s)^2} \tag{22}$$

where N_s is the number of species, M_s and M_r are the molecular weight of species s and r, respectively, γ_s is the molar concentration of species s ($\gamma_s = \rho_s / M_s$), γ_{tot} is the total molar concentration, $\sigma_{sr} = 0.5\ (\sigma_s + \sigma_r)$, where σ_s and σ_r are the effective cross-section of species s and r, respectively, Ω_{sr} and Ω_s are the collision integrals for species s, $\Delta_{sr}^{(1)}$ and $\Delta_{sr}^{(2)}$ are the modified collision integrals for species s, k is the Boltzmann's constant ($k = 1.380622 \times 10^{-23}\,\mathrm{J/K}$) and $\bar{R}$ is the universal gas constant ($\bar{R} = 8314.3\,\mathrm{J/kg - mol\,K}$). $T_{sr} = \sqrt{T_{\varepsilon,s} T_{\varepsilon,r}}$, where $T_{\varepsilon,s}$ and $T_{\varepsilon,r}$ are the effective temperatures for species s and r respectively, given in Table I. $\mu_r = \mu_s$ for species r.

2.3. Source terms

The vibrational/electronic energy source is given by [19]

$$\omega_{\mathrm{v}} = \rho_s \frac{e_{\mathrm{v},s}(T) - e_{\mathrm{v},s}(T_{\mathrm{v}})}{\tau_s} + [e_{\mathrm{v},s}(T_{\mathrm{v}}) + e_{e,s}(T_{\mathrm{v}})]\omega_s \tag{23}$$

where

$$\tau_s = \left(\sum_{r=1}^{N_s} \frac{y_r}{\tau_{sr}} \right)^{-1} \tag{24}$$

$$\tau_{sr} = \frac{\exp[A_{sr}(T^{-1/3} - 0.015B_{sr}^{1/4}) - 18.42]}{p} \tag{25}$$

$$A_{sr} = 1.16 \times 10^{-3} B_{sr}^{0.5} \theta_{\mathrm{v},s}^{4/3}, \quad B_{sr} = \frac{M_s M_r}{M_s + M_r} \tag{26}$$

with y_s being the molar fraction. The pressure, p, in Equation (25) must be inserted in atmospheres to obtain relaxation time in seconds.

The mass rate of production of species s is given by [19]

$$\omega_s = M_s \sum_{r=1}^{N_r} (b_{s,r} - f_{s,r})(R_{\mathrm{f},r} - R_{\mathrm{b},r}) \quad \text{(no summation on } s\text{)} \tag{27}$$

where N_r is the number of reactions, $f_{s,r}$ and $b_{s,r}$ are, respectively, the stoichiometric coefficients for reactants and products in the r reaction, $R_{\mathrm{f},r}$ and $R_{\mathrm{b},r}$ are, respectively, the forward and backward reaction rates for r reaction. These rates are defined by

$$R_{\mathrm{f},r} = k_{\mathrm{f},r} \prod_{s=1}^{N_s} \left(\frac{\rho_s}{M_s} \right)^{f_{s,r}}, \quad R_{\mathrm{b},r} = k_{\mathrm{b},r} \prod_{s=1}^{N_s} \left(\frac{\rho_s}{M_s} \right)^{b_{s,r}} \tag{28}$$

where $k_{\mathrm{f},r}$ and $k_{\mathrm{b},r}$ are the forward and backward reaction rate coefficients, respectively, given by

$$\begin{aligned} k_{\mathrm{f},r} &= C_{\mathrm{f},r} T_x^{n_{\mathrm{f},r}} \exp(-T_d/T_x) \\ k_{\mathrm{b},r} &= \frac{k_{\mathrm{f},r}}{K_{\mathrm{eq},r}} \quad \text{(no summation on } s\text{)} \\ K_{\mathrm{eq},r} &= \exp(B_{1,r} + B_{2,r} \ln Z + B_{3,r} Z + B_{4,r} Z^2 + B_{5,r} Z^3) \end{aligned} \tag{29}$$

where

$$Z = \frac{10^4}{T} \tag{30}$$

The parameters $C_{\mathrm{f},r}$, $n_{\mathrm{f},r}$, T_d, T_x, $B_{1,r}$, $B_{2,r}$, $B_{3,r}$, $B_{4,r}$ and $B_{5,r}$, are those defined by Park [20]. The dissociation reactions are controlled by a combination of the two temperatures, as proposed by Park [20], as follows:

$$T_a = \sqrt{T T_{\mathrm{v}}} \tag{31}$$

3. THE FINITE ELEMENT TAYLOR–GALERKIN SCHEME

3.1. Time discretization: Taylor series

In Taylor–Galerkin scheme, the variables are expanded in time according to a Taylor series, as follows [21]:

$$U^{n+1} = U^n + \Delta t \left(\frac{\partial U}{\partial t}\right)^{n+s_1} + \frac{\Delta t^2}{2}\left(\frac{\partial^2 U}{\partial t^2}\right)^{n+s_2} + \mathrm{O}(\Delta t^3) \tag{32}$$

where the superscript identifies the time step. Thus, one can obtain the results in time step $n+1$ with information from the previous step, n. In addition, the following definitions are given:

$$\begin{aligned} \frac{\partial U^{n+s_1}}{\partial t} &= \frac{\partial U^n}{\partial t} + s_1 \frac{\partial U^{n+1}}{\partial t}, \quad 0 \leqslant s_1 \leqslant 1 \\ \frac{\partial^2 U^{n+s_2}}{\partial t^2} &= \frac{\partial^2 U^n}{\partial t^2} + s_2 \frac{\partial^2 U^{n+1}}{\partial t^2}, \quad 0 \leqslant s_2 \leqslant 1 \end{aligned} \tag{33}$$

Adopting $s_1 = s_2 = 1/2$ and substituting in (32), one obtains

$$\Delta U^{n+1} = \Delta t \left(\frac{\partial U^n}{\partial t} + \frac{1}{2}\frac{\partial \Delta U^{n+1}}{\partial t}\right) + \frac{\Delta t^2}{2}\left(\frac{\partial^2 U^n}{\partial t^2} + \frac{1}{2}\frac{\partial^2 \Delta U^{n+1}}{\partial t^2}\right) + \cdots \tag{34}$$

where $\Delta U^{n+1} = U^{n+1} - U^n$. From Equation (1), the time derivative for U^n is defined as

$$\frac{\partial U^n}{\partial t} = -\frac{\partial F_j^n}{\partial x_j} - \frac{\partial G_j^n}{\partial x_j} - H^n \tag{35a}$$

Similarly, the time derivative for ΔU^{n+1} is defined as

$$\frac{\partial \Delta U^{n+1}}{\partial t} = -\frac{\partial \Delta F_j^{n+1}}{\partial x_j} - \frac{\partial \Delta G_j^{n+1}}{\partial x_j} - \Delta H^{n+1} \tag{35b}$$

Deriving Equation (35a) with respect to t, it is obtained

$$\begin{aligned} \frac{\partial^2 U^n}{\partial t^2} &= \frac{\partial}{\partial t}\left(-\frac{\partial F_j^n}{\partial x_j} - \frac{\partial G_j^n}{\partial x_j} - H^n\right) = \frac{\partial}{\partial x_j}\left(-\frac{\partial F_j^n}{\partial t} - \frac{\partial G_j^n}{\partial t}\right) - \frac{\partial H^n}{\partial t} \\ &= \frac{\partial}{\partial x_j}\left(-\frac{\partial F_j^n}{\partial U}\frac{\partial U^n}{\partial t} - \frac{\partial G_j^n}{\partial U}\frac{\partial U^n}{\partial t}\right) - \frac{\partial H^n}{\partial t} = \frac{\partial}{\partial x_j}\left[(u_j^n + b_j^n)\frac{\partial U^n}{\partial t}\right] - \frac{\Delta H^{n+1}}{\Delta t} \\ &= \frac{\partial}{\partial x_j}\left[-(u_j^n + b_j^n)\left(-\frac{\partial F_k^n}{\partial x_k} - \frac{\partial G_k^n}{\partial x_k} - H^n\right)\right] - \frac{\Delta H^{n+1}}{\Delta t} \end{aligned} \tag{36a}$$

Similarly, the second derivative of ΔU^{n+1} is given by

$$\frac{\partial^2 \Delta U^{n+1}}{\partial t^2} = \frac{\partial}{\partial x_j}\left[-(u_j^n + b_j^n)\left(-\frac{\partial \Delta F_k^{n+1}}{\partial x_k} - \frac{\partial \Delta G_k^{n+1}}{\partial x_k} - \Delta H^{n+1}\right)\right] - \frac{\Delta(\Delta H^{n+1})}{\Delta t} \tag{36b}$$

Substituting Equations (35a), (35b), (36a) and (36b) in Equation (34), neglecting all terms larger in order than second order and introducing an iteration counter, I, for the incremental terms, the following expression is obtained:

$$\Delta U_{I+1}^{n+1} = \Delta t \left[-\frac{\partial F_j^n}{\partial x_j} - \frac{\partial G_j^n}{\partial x_j} - H^n + \frac{\Delta t}{2} \frac{\partial}{\partial x_j} \left(u_j^n \frac{\partial F_k^n}{\partial x_k} \right) \right] + \frac{\Delta t}{2} \left[-\frac{\partial \Delta F_{jI}^{n+1}}{\partial x_j} - \frac{\partial \Delta G_{jI}^{n+1}}{\partial x_j} + \frac{\Delta t}{2} \frac{\partial}{\partial x_j} \left(u_j^n \frac{\partial \Delta F_{kI}^{n+1}}{\partial x_k} \right) \right] \tag{36}$$

where $i, j, k = 1, 2, 3$ and

$$\Delta F_i^{n+1} = F_i^{n+1} - F_i^n, \quad \Delta G_i^{n+1} = G_i^{n+1} - G_i^n \tag{37}$$

3.2. Spatial discretization: Galerkin weighted residual method

Applying the classical Bubnov–Galerkin technique to expression (36) in the context of the finite element method, the following matrix equations are obtained:

(a) Conservation of mass of mixture:

$$\{\Delta\rho\}_{I+1}^{n+1} = \Delta t [M_{\mathrm{L}}]^{-1} \left\{ -[B^C]_i \{F_i^\rho\}^n + \frac{\Delta t}{2} \{f\}^n \right\} + \frac{\Delta t}{2} [M_{\mathrm{L}}]^{-1} \{ -[B^C]_i \{\Delta F_i^\rho\}_I^{n+1} \} \tag{38}$$

(b) Conservation of mass of each species:

$$\{\Delta\rho_s\}_{I+1}^{n+1} = \Delta t [M_{\mathrm{L}}]^{-1} \left\{ -[B^C]_i \{F_i^s\}^n - [K^s]\{y_s\}^n + [M]\{\omega_s\}^n + \frac{\Delta t}{2} \{f\}^n + \{g^s\}^n \right\} + \frac{\Delta t}{2} [M_{\mathrm{L}}]^{-1} \{ -[B^C]_i \{\Delta F_i^\rho\}_I^{n+1} - [K^s]\{\Delta y_s\}_I^{n+1} \} \tag{39}$$

(c) Momentum conservation:

$$\{\Delta\rho u_j\}_{I+1}^{n+1} = \Delta t [M_{\mathrm{L}}]^{-1} \left\{ -[B^C]_i \{F_{ij}^u\}^n - [D]_{ij} \{u_j\}^n + \frac{\Delta t}{2} \{f\}^n + \{g^u\}^n \right\} + \frac{\Delta t}{2} [M_{\mathrm{L}}]^{-1} \{ -[B^C]_i \{\Delta F_i^\rho\}_I^{n+1} - [D]_{ij} \{\Delta u_i\}_I^{n+1} \} \tag{40}$$

(d) Vibrational energy conservation:

$$\{\Delta\rho e_{\mathrm{v}}\}_{I+1}^{n+1} = \Delta t [M_{\mathrm{L}}]^{-1} \{ -[B^C]_i \{F_i^{\mathrm{v}}\}^n - [K^{\mathrm{v}}]\{T_{\mathrm{v}}\}^n - [K^{s\mathrm{v}}]\{y_s\}^n - [M]\{\omega_{\mathrm{v}}\}^n + \frac{\Delta t}{2} \{f\}^n + \{g^{\mathrm{v}}\}^n \} + \frac{\Delta t}{2} [M_{\mathrm{L}}]^{-1} \{ -[B^C]_i \{\Delta F_i^e\}_I^{n+1} - [K^{\mathrm{v}}]\{\Delta T_{\mathrm{v}}\}_I^{n+1} - [K^{s\mathrm{v}}]\{\Delta y_s\}_I^{n+1} \} \tag{41}$$

(e) Total energy conservation:

$$\{\Delta\rho e\}_{I+1}^{n+1} = \Delta t[M_{\mathrm{L}}]^{-1}\{-[B^C]_i\{F_i^e\}^n - [E]_i\{u_i\}^n - [K^{\mathrm{v}}]\{T_{\mathrm{v}}\}^n - [K^e]\{T\}^n - [K^{se}]\{y_s\}^n + \frac{\Delta t}{2}\{f\}^n + \{g^e\}^n\} + \frac{\Delta t}{2}[M_{\mathrm{L}}]^{-1}\{-[B^C]_i\{\Delta F_i^e\}_I^{n+1} - [K^{\mathrm{v}}]\{\Delta T_{\mathrm{v}}\}_I^{n+1} - [K^e]\{\Delta T\}_I^{n+1} - [K^{se}]\{\Delta y_s\}_I^{n+1}\} \tag{42}$$

where

$$[M] = \int_{\Omega_e} [\Phi]^{\mathrm{T}}[\Phi]\,\mathrm{d}\Omega \tag{43}$$

$$[M_{\mathrm{L}}] = \begin{cases} \Omega_e/8 & \text{for main diagonal elements} \\ 0 & \text{for all off-diagonal elements} \end{cases} \tag{44}$$

$$[B^C]_i = \int_{\Omega_e} [\Phi]^{\mathrm{T}} \frac{\partial[\Phi]}{\partial x_i}\,\mathrm{d}\Omega + \frac{\Delta t}{2}\int_{\Omega_e} ([\Phi]\{u_k\}^n)\frac{\partial[\Phi]}{\partial x_i}^{\mathrm{T}} \frac{\partial[\Phi]}{\partial x_i}\,\mathrm{d}\Omega \tag{45}$$

$$[D]_{ij} = \begin{cases} \displaystyle\int_{\Omega_e} \mu\left(2+\frac{\mu}{\lambda}\right)\frac{\partial[\Phi]^{\mathrm{T}}}{\partial x_i}\frac{\partial[\Phi]}{\partial x_i}\,\mathrm{d}\Omega \\ \quad \displaystyle + \int_{\Omega_e} \mu \frac{\partial[\Phi]^{\mathrm{T}}}{\partial x_k}\frac{\partial[\Phi]}{\partial x_k}\,\mathrm{d}\Omega \qquad \text{if } i=j \text{ and } \begin{cases} i=1\to k=2,3 \\ i=2\to k=1,3 \\ i=3\to k=1,2 \end{cases} \\ \displaystyle\int_{\Omega_e} \mu \frac{\partial[\Phi]^{\mathrm{T}}}{\partial x_i}\frac{\partial[\Phi]}{\partial x_j}\,\mathrm{d}\Omega \\ \quad \displaystyle + \int_{\Omega_e} \lambda \frac{\partial[\Phi]^{\mathrm{T}}}{\partial x_j}\frac{\partial[\Phi]}{\partial x_i}\,\mathrm{d}\Omega \qquad \text{if } i\neq j \end{cases} \tag{46}$$

$$[E]_i = \int_{\Omega_e} \left[\mu([\Phi]\{u_i\}^n)\frac{\partial[\Phi]^{\mathrm{T}}}{\partial x_k}\frac{\partial[\Phi]}{\partial x_k} + \mu([\Phi]\{u_k\}^n)\frac{\partial[\Phi]^{\mathrm{T}}}{\partial x_i}\frac{\partial[\Phi]}{\partial x_k} + \lambda([\Phi]\{u_k\}^n)\frac{\partial[\Phi]^{\mathrm{T}}}{\partial x_k}\frac{\partial[\Phi]}{\partial x_i}\right]\mathrm{d}\Omega \tag{47}$$

$$[K^{\mathrm{v}}] = \int_{\Omega_e} \eta_{\mathrm{v}} \frac{\partial[\Phi]^{\mathrm{T}}}{\partial x_i}\frac{\partial[\Phi]}{\partial x_i}\,\mathrm{d}\Omega \tag{48}$$

$$[K^e] = \int_{\Omega_e} \eta \frac{\partial[\Phi]^{\mathrm{T}}}{\partial x_i}\frac{\partial[\Phi]}{\partial x_i}\,\mathrm{d}\Omega \tag{49}$$

$$[K^s] = \int_{\Omega_e} D_s([\Phi]\{\rho\}^n)\frac{\partial[\Phi]^{\mathrm{T}}}{\partial x_i}\frac{\partial[\Phi]}{\partial x_i}\,\mathrm{d}\Omega \tag{50}$$

$$[K^{sv}] = \int_{\Omega_e} h_{v,s} D_s([\Phi]\{\rho\}^n) \frac{\partial[\Phi]^T}{\partial x_i} \frac{\partial[\Phi]}{\partial x_i} \, d\Omega \tag{51}$$

$$[K^{se}] = \int_{\Omega_e} h_s D_s([\Phi]\{\rho\}^n) \frac{\partial[\Phi]^T}{\partial x_i} \frac{\partial[\Phi]}{\partial x_i} \, d\Omega \tag{52}$$

$$\{f\}^n = \int [\Phi^*]^T ([\Phi]\{u_k\}^n) n_k \left(\frac{\partial[\Phi]}{\partial x_i} \{F_i\}^n \right) d\Gamma \tag{53}$$

$$\{g^s\}^n = \int_{\Gamma_e} [\Phi^*]^T D_s([\Phi]\{\rho\}^n) \left(\frac{\partial[\Phi]}{\partial x_i} \{y_s\} \right) n_i \, d\Gamma \tag{54}$$

$$\{g_j^u\}^n = \int_{\Gamma_e} [\Phi^*]^T \left[\mu \left(\frac{\partial[\Phi]}{\partial x_i} \{u_j\}^n + \frac{\partial[\Phi]}{\partial x_j} \{u_i\}^n \right) + \lambda \left(\frac{\partial[\Phi]}{\partial x_k} \{u_k\}^n \right) \delta_{ij} \right] n_i \, d\Gamma \tag{55}$$

$$\{g^v\}^n = \int_{\Gamma_e} [\Phi^*]^T \left[\eta_v \left(\frac{\partial[\Phi]}{\partial x_i} \{T_v\} \right) + h_{v,s} D_s([\Phi]\{\rho\}^n) \left(\frac{\partial[\Phi]}{\partial x_i} \{y_s\} \right) \right] n_i \, d\Gamma \tag{56}$$

$$\{g^e\}^n = \int_{\Gamma_e} [\Phi^*]^T \left\{ \eta_v \left(\frac{\partial[\Phi]}{\partial x_i} \{T_v\} \right) + \eta \left(\frac{\partial[\Phi]}{\partial x_i} \{T\} \right) + h_s D_s([\Phi]\{\rho\}^n) \left(\frac{\partial[\Phi]}{\partial x_i} \{y_s\} \right) + ([\Phi]\{u_j\}^n) \left[\mu \left(\frac{\partial[\Phi]}{\partial x_i} \{u_j\}^n + \frac{\partial[\Phi]}{\partial x_j} \{u_i\}^n \right) + \lambda \left(\frac{\partial[\Phi]}{\partial x_k} \{u_k\}^n \right) \delta_{ij} \right] \right\} n_i \, d\Gamma \tag{57}$$

In these expressions, Ω_e and Γ_e are the element volume and the boundary surface, respectively, $[\Phi]$ is the vector containing the shape functions for each node, $[\Phi^*]$ is the vector containing the shape functions evaluated on the contour surface and $[M_L]$ is the lumped mass matrix.

After assembling Equations (38)–(42) and applying the corresponding boundary conditions, the nodal values of ρ, ρ_s, ρu_j, ρe_v and ρe can be computed at each time level by using an iterative scheme. Nodal values of thermodynamic pressure are calculated with the equation of state, Equation (3).

The Courant–Friedrichs–Lewy (CFL) stability condition for each element is given by

$$\Delta t_e = \beta \frac{L_e}{a + \sqrt{u_i u_i}} \tag{58}$$

where L_e is a characteristic dimension for the element, a is the speed of sound and β is a safety coefficient (in this work, $\beta = 0.3$ was adopted). Equations (39)–(43) were applied with a uniform value of Δt on the whole finite element mesh. The smallest value of Δt_e obtained by applying the above equation to all elements was adopted.

To capture strong discontinuities and eliminate high-frequency oscillations near shock waves, an artificial viscosity is used. The smoothed solution is obtained from the non-smoothed solution by applying the following expression:

$$\{U_s\}^{n+1} = \{U\}^{n+1} + [M_L]^{-1}\{D\}^n \tag{59}$$

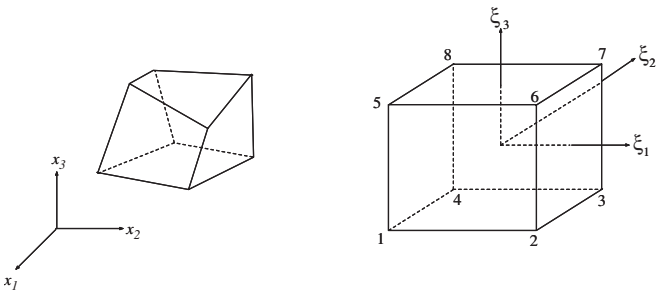

Figure 1. Physical and computational spaces for the eight-node hexahedral isoparametric element.

where the artificial damping vector is given by

$$\{D\}^n = \sum C_e C_{\text{ad}} S_e([M] - [M_{\text{L}}])_e \{U\}^n \tag{60}$$

In the above equation, $C_e = \Delta t/\Delta t_e$ is the local Courant number, C_{ad} is an artificial damping coefficient given by the user (in this work, $C_{\text{ad}} = 2.0$ for non-viscous fluids and $C_{\text{ad}} = 1.0$ for viscous fluids), and S_e is a pressure sensor at element level obtained as an average of nodal values S_N. Values of S_N are components of the following assembled global vector:

$$\{S\}^n = \frac{\sum_e |([M] - [M_{\text{L}}])_e \{p\}_e^n|}{\sum_e |([M] - [M_{\text{L}}])_e |\{p\}_e^n} \tag{61}$$

where the bars indicate that absolute values of the corresponding terms must be taken. This approach was previously used by Argyris *et al.* [15].

3.3. Analytical evaluation of element matrices

In this work, the eight-node hexahedral isoparametric element has been used. In Figure 1 the element is shown in its physical and computational spaces.

The shape functions for each node are given by

$$\Phi_N = \tfrac{1}{8}[1 + \xi_{1N}\xi_1][1 + \xi_{2N}\xi_2][1 + \xi_{3N}\xi_3], \quad N = 1, 2, \ldots, 8 \tag{62}$$

where ξ_{iN} are the natural co-ordinates of node N.

The shape function derivatives with respect to the global co-ordinates x_i are given by

$$\frac{\partial[\Phi]}{\partial x_j} = J_{ij}^{-1} \frac{\partial[\Phi]}{\partial \xi_i} \tag{63}$$

where J_{ij}^{-1} are the components of the inverse of the Jacobian matrix J, which can be written as

$$J(\xi_1,\xi_2,\xi_3)=\begin{bmatrix}J_{11} & J_{12} & J_{13}\\ J_{21} & J_{22} & J_{23}\\ J_{31} & J_{32} & J_{33}\end{bmatrix}=\begin{bmatrix}\dfrac{\partial[\Phi]}{\partial\xi_1}\{x_1\} & \dfrac{\partial[\Phi]}{\partial\xi_1}\{x_2\} & \dfrac{\partial[\Phi]}{\partial\xi_1}\{x_3\}\\ \dfrac{\partial[\Phi]}{\partial\xi_2}\{x_1\} & \dfrac{\partial[\Phi]}{\partial\xi_2}\{x_2\} & \dfrac{\partial[\Phi]}{\partial\xi_2}\{x_3\}\\ \dfrac{\partial[\Phi]}{\partial\xi_3}\{x_1\} & \dfrac{\partial[\Phi]}{\partial\xi_3}\{x_2\} & \dfrac{\partial[\Phi]}{\partial\xi_3}\{x_3\}\end{bmatrix} \tag{64}$$

where $\{x_i\}$ are the vectors containing the global co-ordinates of the eight nodes of the element.

The differential volume is $\mathrm{d}\Omega=|J|\,\mathrm{d}\xi_1\,\mathrm{d}\xi_2\,\mathrm{d}\xi_3$, where $|J|$ is the determinant of the Jacobian matrix J.

Using Equations (62)–(64) in Equations (43)–(57), evaluating the inverse and the determinant of the Jacobian matrix at the element centre (where $\xi_1=\xi_2=\xi_3=0$), and solving the integrals given in Equations (43)–(57), the following analytical expressions are obtained for the element matrices:

$$M_{MN}=\frac{\Omega_e}{64}\left(1+\frac{1}{3}\,\xi_{1M}\xi_{1N}\right)\left(1+\frac{1}{3}\,\xi_{2M}\xi_{2N}\right)\left(1+\frac{1}{3}\,\xi_{3M}\xi_{3N}\right) \tag{65}$$

$$M_{\mathrm{L}MN}=\frac{\Omega_e}{8}\,\delta_{MN} \tag{66}$$

$$\begin{aligned}B_{iMN}=\frac{1}{8}\Bigg[&\bar{J}_{i1}(0)\xi_{1N}\left(1+\frac{1}{3}\,\xi_{2M}\xi_{2N}\right)\left(1+\frac{1}{3}\,\xi_{3M}\xi_{3N}\right)\\ &+\bar{J}_{i2}(0)\xi_{2N}\left(1+\frac{1}{3}\,\xi_{1M}\xi_{1N}\right)\left(1+\frac{1}{3}\,\xi_{3M}\xi_{3N}\right)\\ &+\bar{J}_{i3}(0)\xi_{3N}\left(1+\frac{1}{3}\,\xi_{1M}\xi_{1N}\right)\left(1+\frac{1}{3}\,\xi_{2M}\xi_{2N}\right)\Bigg]\end{aligned} \tag{67}$$

where the components of the matrix $\bar{J}(0)$ are given by

$$\bar{J}(0)=\begin{bmatrix}[J_{22}J_{33}-J_{23}J_{32}]_{(0)} & [J_{13}J_{32}-J_{12}J_{33}]_{(0)} & [J_{12}J_{23}-J_{13}J_{22}]_{(0)}\\ [J_{23}J_{31}-J_{21}J_{31}]_{(0)} & [J_{11}J_{33}-J_{13}J_{31}]_{(0)} & [J_{31}J_{21}-J_{11}J_{23}]_{(0)}\\ [J_{21}J_{32}-J_{22}J_{31}]_{(0)} & [J_{12}J_{31}-J_{11}J_{32}]_{(0)} & [J_{11}J_{22}-J_{12}J_{21}]_{(0)}\end{bmatrix} \tag{68}$$

Thus, from Equation (46), the following expression can be obtained:

$$C_{iMN}=\left(\frac{1}{8}\sum_{M=1}^{8}u_{kM}^{n}\right)\frac{1}{\Omega_e}\,a_{kiMN} \tag{69}$$

where

$$a_{kiMN}=\bar{J}_{kj}(0)\bar{J}_{ih}(0)A_{jhMN} \tag{70}$$

with the factor A_{jhMN} being defined as follows:

$$A_{ijMN} = \begin{cases} \xi_{iM}\xi_{jN}\left(1+\dfrac{1}{3}\,\xi_{kM}\xi_{kN}\right) & \text{if } i\neq j \text{ and } \begin{cases} \text{if } i=1 \text{ and } j=2 \to k=3 \\ \text{if } i=2 \text{ and } j=3 \to k=1 \\ \text{if } i=3 \text{ and } j=1 \to k=2 \end{cases} \\ \xi_{iM}\xi_{jN}\left(1+\dfrac{1}{3}\,\xi_{kM}\xi_{kN}\right) & \\ \quad\times\left(1+\dfrac{1}{3}\xi_{hM}\xi_{hN}\right) & \text{if } i=j \text{ and } \begin{cases} \text{if } i=j=1 \to k=2 \text{ and } h=3 \\ \text{if } i=j=2 \to k=1 \text{ and } h=3 \\ \text{if } i=j=3 \to k=1 \text{ and } h=2 \end{cases} \end{cases} \tag{71}$$

Thus, the diffusion matrix becomes

$$\begin{aligned} D_{ijMN} &= \frac{1}{\Omega_e}[\mu a_{ijMN} + \lambda a_{jiMN}] && \text{if } i\neq j \\ D_{iiMN} &= \frac{1}{\Omega_e}[(2\mu+\lambda)a_{iiMN} + \mu a_{kkMN}] && \text{if } i=j \text{ and } \begin{cases} \text{if } i=1 \to k=2,3 \\ \text{if } i=2 \to k=1,3 \\ \text{if } i=3 \to k=1,2 \end{cases} \end{aligned} \tag{72}$$

$$E_{iMN} = \frac{1}{\Omega_e}\left[\mu\left(\frac{1}{8}\sum_{M=1}^{8} u_{iM}\right)a_{iiMN} + \mu\left(\frac{1}{8}\sum_{M=1}^{8} u_{jM}\right)a_{ijMN} + \lambda\left(\frac{1}{8}\sum_{M=1}^{8} u_{jM}\right)a_{jiMN}\right] \tag{73}$$

and

$$K_{MN} = \frac{1}{\Omega_e}\,K a_{iiMN} \tag{74}$$

In expressions (65)–(74), M and N are nodal indexes and $M,N=1,2,\ldots,8$, whereas $i,j,k,h=1,2,3$.

To simplify the analytical solution of the boundary integrals at the element level of Equations (53)–(57), average values of element actions are considered on the corresponding boundary element faces, and these actions are assumed to be uniformly distributed on the four nodes belonging to each boundary face. With this simplification, the following equivalent vectors due to boundary actions are obtained:

$$\{f\}^n = \frac{1}{4}\,(u_k^n|_0 n_k)\left(\frac{1}{8}\sum_{N=1}^{8}\xi_{kN}J_{ik}^{-1}F_{iN}^n\right)\{\Xi\}\int_{\Gamma_e}\mathrm{d}\Gamma \tag{75}$$

$$\{g^s\}^n = \frac{1}{4}\,D_s(\rho^n|_0 n_k)\left(\frac{1}{8}\sum_{N=1}^{8}\xi_{kN}J_{ik}^{-1}y_N^n\right)\{\Xi\}\int_{\Gamma_e}\mathrm{d}\Gamma \tag{76}$$

$$\{g_j^u\}^n = \frac{1}{4}\tau_{ij}^n|_0\, n_i\{\Xi\}\int_{\Gamma_e}\mathrm{d}\Gamma \tag{77}$$

$$\{g^{\mathrm{v}}\}^n = \frac{1}{4}\left[\eta_{\mathrm{v}}\left(\frac{1}{8}\sum_{N=1}^{8}\xi_{kN}J_{ik}^{-1}T_{\mathrm{v}N}^n\right)n_i + h_{\mathrm{v},s}D_s(\rho^n|_0 n_k)\left(\frac{1}{8}\sum_{N=1}^{8}\xi_{kN}J_{ik}^{-1}y_N^n\right)\right]\{\Xi\}\int_{\Gamma_e}\mathrm{d}\Gamma \tag{78}$$

$$\{g^e\}^n = \frac{1}{4} u_j^n|_0 \tau_{ij}^n|_0 n_i \{\Xi\} \int_{\Gamma_e} \mathrm{d}\Gamma + \frac{1}{4} \left[\eta_\mathrm{v} \left(\frac{1}{8} \sum_{N=1}^{8} \xi_{kN} J_{ik}^{-1} T_{\mathrm{v}N}^n \right) n_i + \eta \left(\frac{1}{8} \sum_{N=1}^{8} \xi_{kN} J_{ik}^{-1} T_N^n \right) n_i + h_s D_s (\rho^n|_0 n_k \left(\frac{1}{8} \sum_{N=1}^{8} \xi_{kN} J_{ik}^{-1} y_N^n \right) \right] \{\Xi\} \int_{\Gamma_e} \mathrm{d}\Gamma \quad (79)$$

where

$$\rho^n|_0 = \frac{1}{8} \sum_{N=1}^{8} \rho_N^n \quad (80)$$

$$u_j^n|_0 = \frac{1}{8} \sum_{N=1}^{8} u_{jN}^n \quad (81)$$

$$\tau_{ij}^n|_0 = \frac{\mu}{8} \left(\sum_{N=1}^{8} \xi_{kN} J_{ik}^{-1} u_{jN}^n + \sum_{N=1}^{8} \xi_{kN} J_{jk}^{-1} u_{iN}^n \right) + \frac{\lambda}{8} \left(\sum_{N=1}^{8} \xi_{kN} J_{lk}^{-1} u_{lN}^n \right) \quad (82)$$

are the average values of the density, velocity and viscous shear stresses on the boundary element, respectively. Finally,

$$\Xi_N = \begin{cases} 1 & \text{if } N \text{ is a boundary node} \\ 0 & \text{if } N \text{ is not a boundary node} \end{cases} \quad (83)$$

4. NUMERICAL RESULTS

4.1. Nitrogen flow over an half-cylinder

The non-diffusive hypersonic flow of nitrogen partially dissociated over a half-cylinder with 25.4 mm radius is analysed, which can be schematically seen in Figure 2. The free flow conditions are Mach = 6.13, temperature = 1833 K, velocity = 5590 m/s, density = 5.349×10^{-3} kg/m^3 and atomic nitrogen mass fraction = 0.073. This problem was analysed experimentally by Hornung [22]. The five-species model is employed, but three species (O_2, NO and O) are neglected in order to perform this 2-species problem (N_2 and N).

Owing to symmetry, only the upper half of the cylinder is analysed. Since this is a two-dimensional problem, but the code solves 3D problems, only one element is used in the x_3 direction ($\Delta x_3 = 0.005$ m). The finite element mesh is constituted of 1500 elements ($50 \times 30 \times 1$ elements) with 3162 nodes and is shown in Figure 3(a).

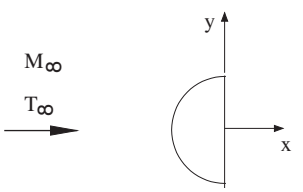

Figure 2. Sketch of the nitrogen flow over an half-cylinder.

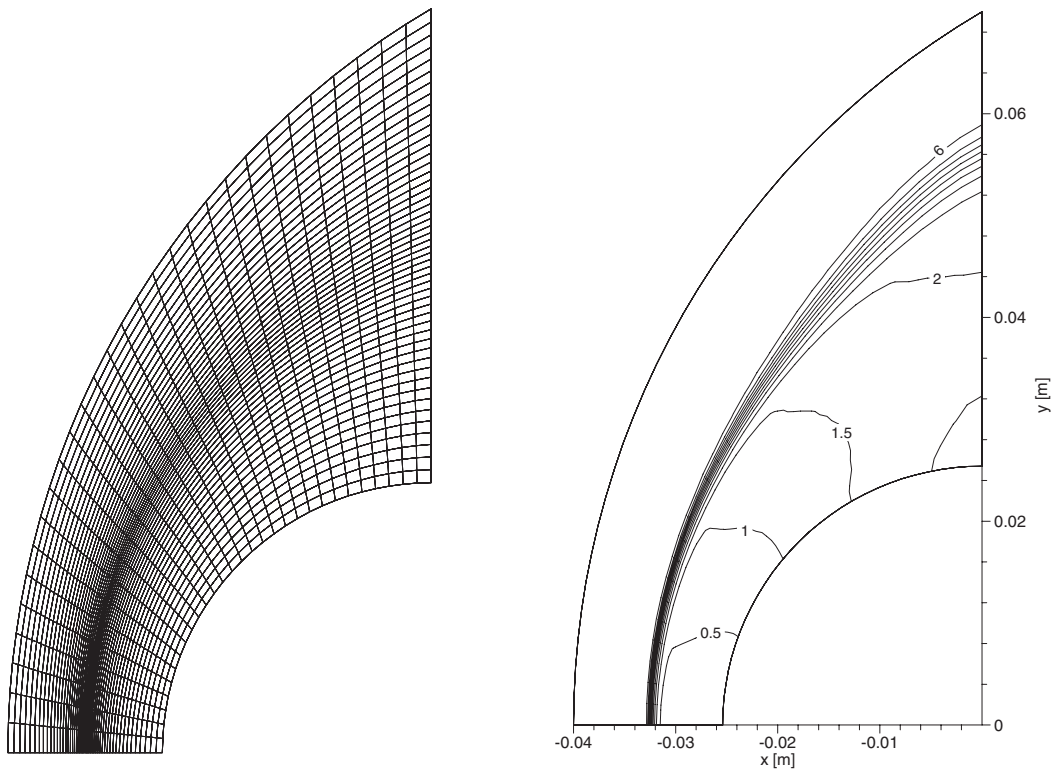

(a) (b)

Figure 3. Finite element mesh (a) and Mach number contours (b).

The Mach number contours are shown in Figure 3(b). In Figures 4(a) and 4(b) the temperatures and mass fraction distributions along the stagnation line, respectively, are shown. The numerical result for the shock position obtained by the present work agrees with the experimental result obtained by Hornung [22], as can be seen in Figure 4(a). The result for perfect gas model fails to find the correct position of the shock. Furthermore, the temperature for perfect gas model remains practically unchanged between the shock and the cylinder's surface, while for the model with high temperature effects, the temperatures distributions have a maximum peak just after the shock and they continuously decrease towards the cylinder surface. This effect is explained by the chemical reactions, since dissociation is endothermic. In Figure 4(b), it is shown that the mass fraction distributions along the stagnation line are less steep than the temperature ones. This phenomenon was expected, since chemical reactions need a large number of collisions to occur.

4.2. Hypersonic flow of air around a half-ellipse

Non-diffusive hypersonic flow of air in thermal equilibrium around a half-ellipse travelling at an altitude of 75 km is analysed, which can be schematically seen in Figure 5.

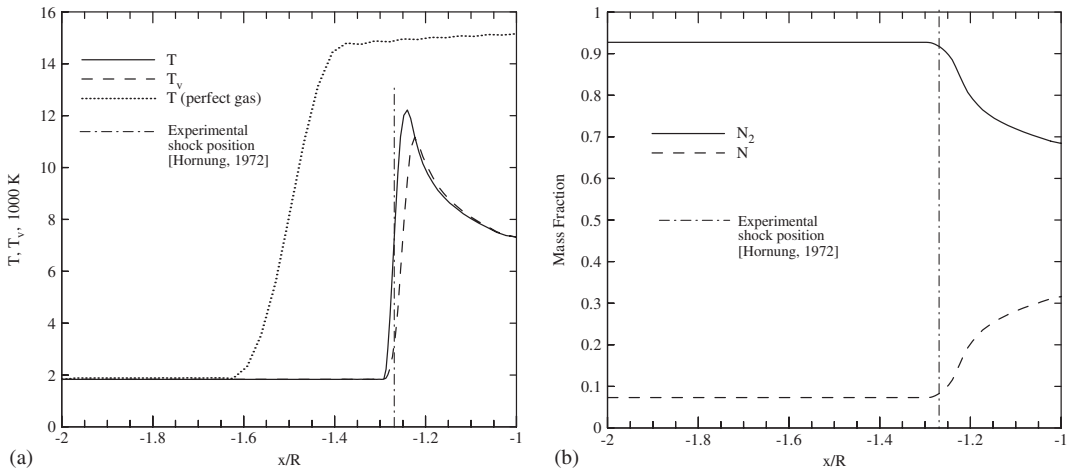

Figure 4. Temperature (a) and mass fractions (b) distributions along the stagnation line.

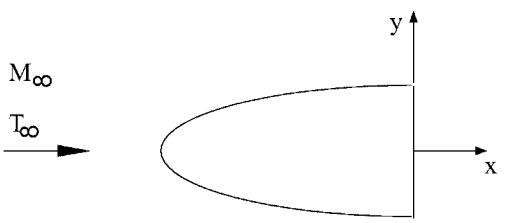

Figure 5. Sketch of the air flow over an half-ellipse.

The semi-axis of the ellipse are $a = 6.0$ cm and $b = 1.5$ cm. The free stream conditions are: Mach number $= 25$, velocity $= 7250$ m/s, temperature $= 208.399$ K, pressure $= 2.388$ Pa, density $= 3.991 \times 10^{-5}$ kg/m^3, mass fraction of molecular nitrogen $= 0.767$, mass fraction of molecular oxygen $= 0.233$, mass fraction of the other three species $= 0$. This problem was analysed by Argyris *et al.* [14, 16].

Owing to symmetry, only the upper half of the ellipse is analysed. Since this is also a two-dimensional problem, only one element is used in x_3 direction ($\Delta x_3 = 0.005$ m). The finite element mesh is constituted of 3600 elements ($60 \times 60 \times 1$ elements) with 7442 nodes and is shown in Figure 6.

In Figures 7(a) and 7(b) are shown the Mach number and the temperature contours, respectively. Figures 8(a), 8(b), 9(a) and 9(b) show the results obtained in the present work and those obtained by Argyris *et al.* [14, 16] for temperature, pressure, mixture density and mass fractions distributions along stagnation line, respectively. It can be seen that the results of this work are in good agreement with those of Argyris *et al.* [14, 16].

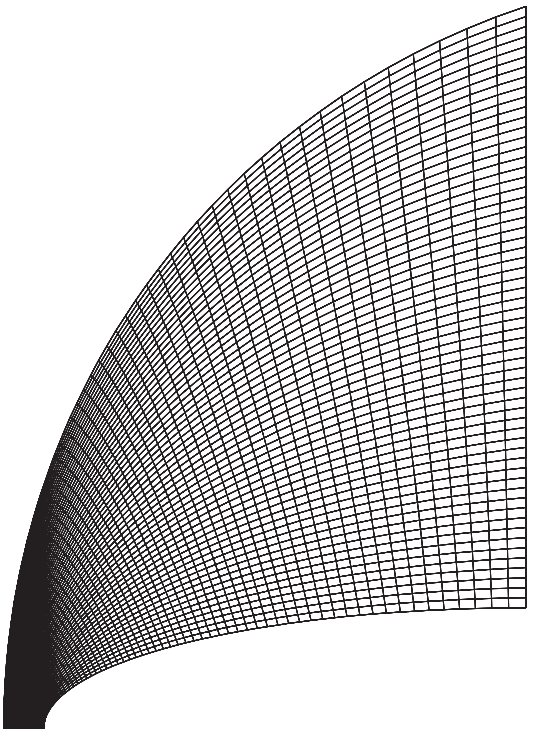

Figure 6. Finite element mesh for the ellipse problem.

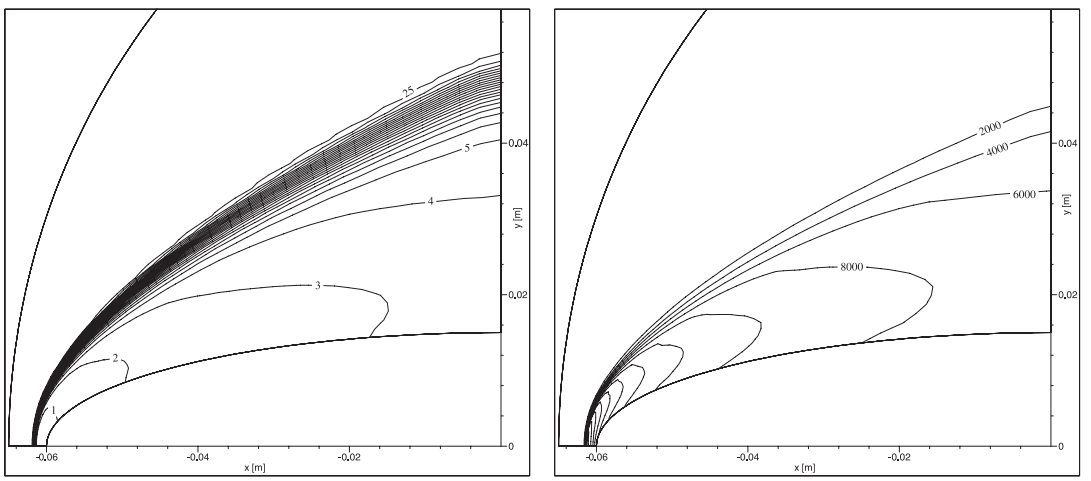

(a) (b)

Figure 7. Mach number (a) and temperature (b) contours.

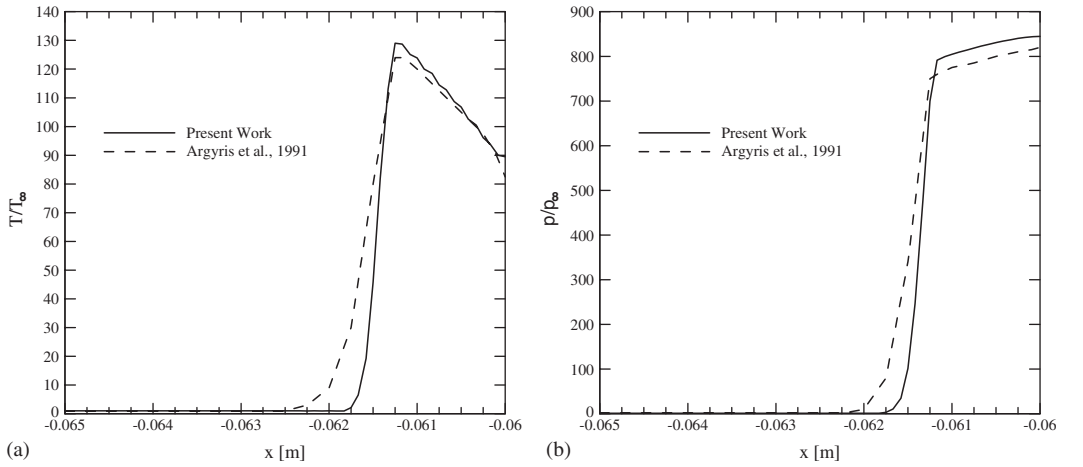

Figure 8. Variation of temperature (a) and of pressure (b) along the stagnation line.

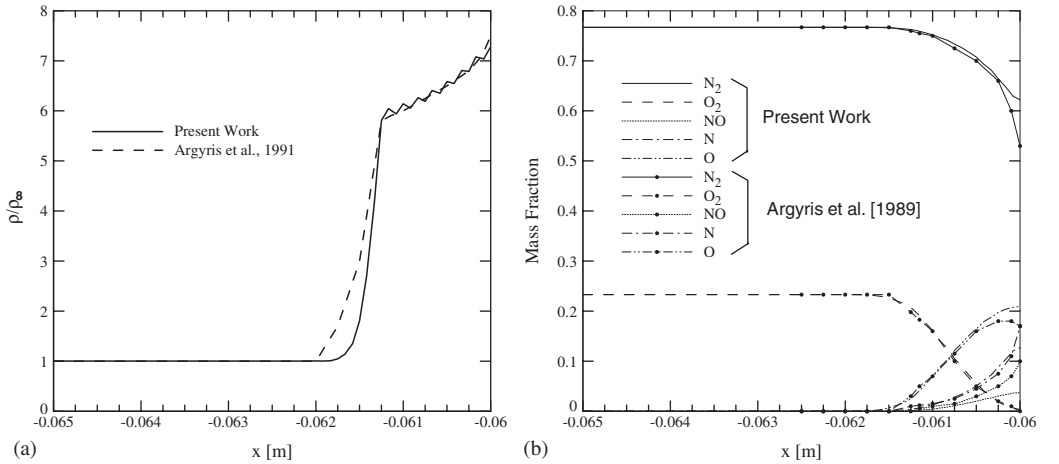

Figure 9. Variation of density (a) and mass fractions (b) along the stagnation line.

4.3. Diffusive hypersonic flow around an half-sphere

The diffusive hypersonic flow of air partially dissociated around an half-sphere with 2 cm of radius is analysed, which can be schematically seen in Figure 10. The free stream conditions are: Mach number $= 11.16$, velocity $= 5940$ m/s, temperature $= 705$ K, density $= 1.56 \times 10^{-3}$, $\mathrm{Re}_\infty = 1.14 \times 10^4$, mass fractions of N_2, O_2, NO, N and O are, respectively, 0.762, 0.035, 0.032, 0 and 0.171.

To reduce the computational cost, only one-fourth of the half-sphere is analysed. The finite element mesh is constituted of 36771 nodes and 33 750 elements and is shown in Figure 11(a).

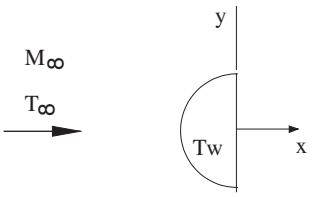

Figure 10. Sketch of the air flow around an half-sphere.

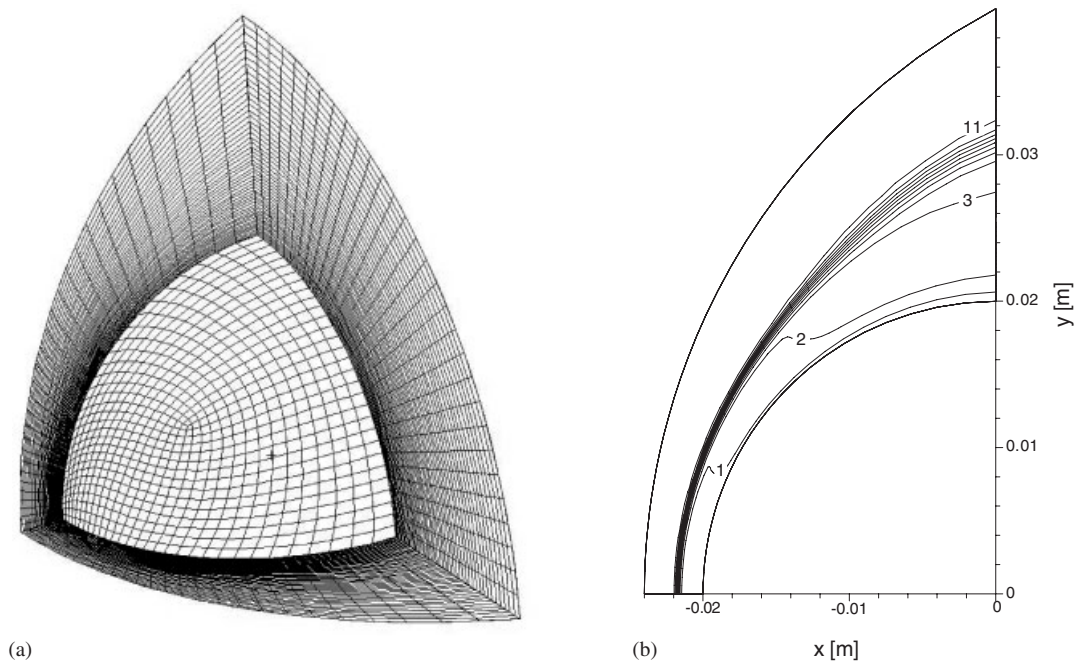

Figure 11. Finite element mesh (a) and Mach number contours (b).

In Figure 11(b) is shown the Mach number contour. Translational and vibrational temperatures contours are shown in Figures 12(a) and 12(b), respectively. In Figure 13(a) are shown the Mach number, the translational and vibrational temperatures distributions along the stagnation line. In Figure 13(b) are shown the mass fractions distributions along the stagnation line.

5. CONCLUSIONS

The numerical procedure proposed by the present work reproduces the experimental shock position for the nitrogen flow around a cylinder. In addition, the results obtained in the present

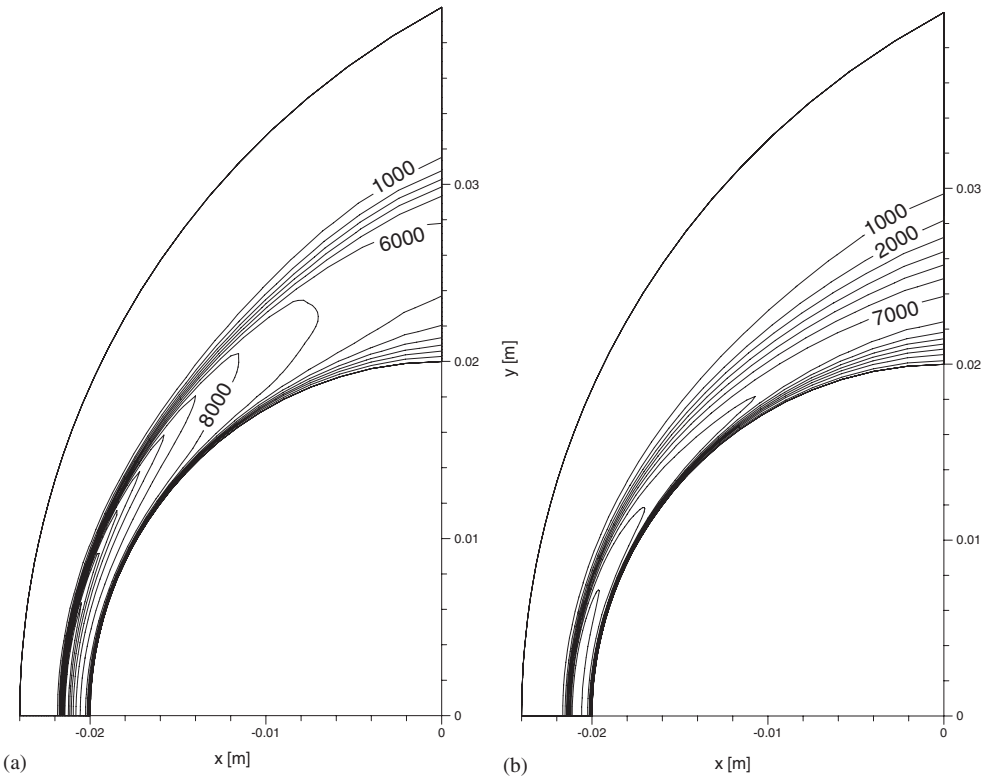

Figure 12. Translational (a) and vibrational (b) temperatures contours (K).

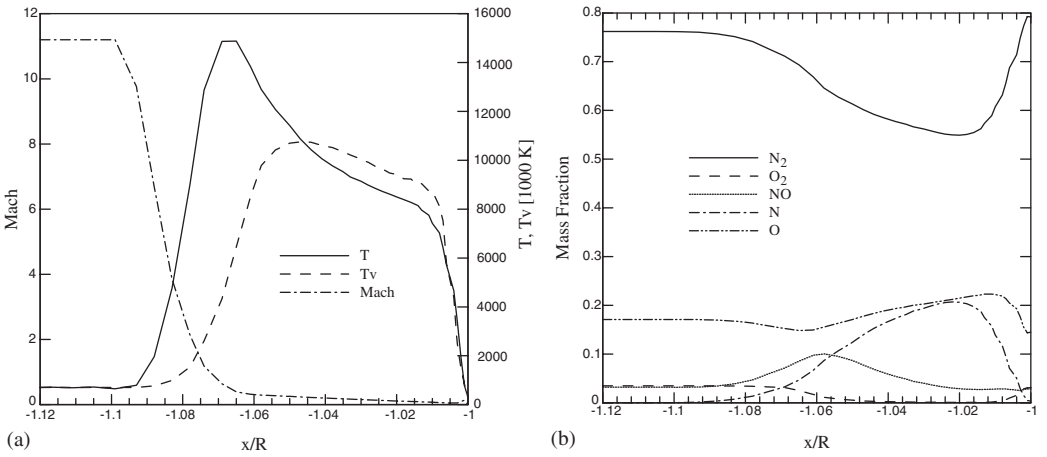

Figure 13. Mach number and temperatures (a) and mass fractions (b) along the stagnation line.

work for the problem of hypersonic flow around an half-ellipse are in good agreement with those obtained numerically by Argyris *et al.* [14, 16]. In all examples, the mass fractions of chemical species usually take more time to respond to the shock than the other properties (e.g. temperature). This phenomenon was expected since chemical reactions require a large number of collisions to occur, which demands certain amount of time. The vibrational temperature usually presents smaller values and respond a little later to the shock than the translational temperature. This was also expected since the molecules become vibrationally excited only above a specific temperature (typically, 800 K for air at 1 atm). Future works will include adaptive meshes as well as ionization processes.

ACKNOWLEDGEMENTS

The authors wish to thank the National Supercomputing Center of the Federal University of Rio Grande do Sul and the Brazilian Space Agency for their support.

REFERENCES

1. Anderson JD. *Hypersonic and High Temperature Gas Dynamics*. McGraw-Hill: New York, 1989.
2. Brown KG. Chemical and thermal nonequilibrium heat-transfer analysis for hypervelocity, low Reynolds number flow. In *Thermophysical Aspects of Re-Entry Flows*, Moss JN, Scott CD (eds). AIAA: New York, 1986; 445–477.
3. Park C. *Nonequilibrium Hypersonic Aerothermodynamics*. Wiley: New York, 1990.
4. Lee JH. Basic governing equations for the flight regimes of aeroassisted orbital transfer vehicles. In *Thermal Design of Aeroassisted Orbital Transfer Vehicles*, Nelson HF (ed.). AIAA: New York, 1985; 3–53.
5. Park C. Problems of Rate Chemistry in the Flight Regimes of Aeroassisted Orbital Transfer Vehicles. In *Thermal Design of Aeroassisted Orbital Transfer Vehicles*, Nelson HF (ed.). AIAA: New York, 1985; 511–537.
6. Moretti G, Abbett M. A time-dependent computational method for blunt body flows. *AIAA Journal* 1966; **4**(12):2136–2141.
7. Lax P, Wendroff B. Systems of conservation laws. *Communications on Pure and Applied Mathematics* 1960; **13**:217–237.
8. Lax P, Wendroff B. On the Stability of Difference Schemes. *Communications on Pure and Applied Mathematics* 1962; **15**:363–371.
9. Lax P, Wendroff B. Difference schemes for hyperbolic equations with high order accuracy. *Communications on Pure and Applied Mathematics* 1964; **17**:381–398.
10. Désidéri JA. The computation over unstructured grids of inviscid hypersonic reactive flow by upwind finite-volume schemes. In *Computational Methods in Hypersonic Aerodynamics*, Murthy TKS (ed.). Kluwer Academic Publishers: Dordrecht, 1991; 387–446.
11. Donea J. A Taylor–Galerkin method for convective transport problems. *International Journal for Numerical Methods in Engineering* 1984; **20**:101–119.
12. Codina R. Comparison of some finite element methods for solving the diffusion–convection–reaction equation. *Computer Methods in Applied Mechanics and Engineering* 1998; **156**:185–210.
13. Safjan A, Oden JT. High-order Taylor–Galerkin methods for linear hyperbolic systems. *Journal of Computational Physics* 1995; **120**:206–230.
14. Argyris J, Doltsinis IS, Friz H. Hermes space shuttle: explorations of reentry aerodynamics. *Computer Methods in Applied Mechanics and Engineering* 1989; **73**:1–51.
15. Argyris J, Doltsinis IS, Friz H. Studies on computational reentry aerodynamics. *Computer Methods in Applied Mechanics and Engineering* 1990; **81**:257–289.
16. Argyris J, Doltsinis IS, Friz H, Urban J. An exploration of chemically reacting viscous hypersonic flow. *Computer Methods in Applied Mechanics and Engineering* 1991; **89**:85–128.
17. Argyris J, Doltsinis IS, Friz H, Urban J. Physical and computational aspects of chemically reacting hypersonic flows. *Computer Methods in Applied Mechanics and Engineering* 1994; **111**:1–35.
18. Bird RB, Stewart WE, Lightfoot EN. *Transport Phenomena*. Wiley: New York, 1960.
19. Gnoffo PA, Gupta ON, Shinn JL. Conservation equations and physical models for hypersonic air flows in thermal and chemical nonequilibrium. *NASA* TP-2867, 1989.

20. Park C. Convergence of computation of chemical reacting flows. In *Thermophysical Aspects of Re-Entry Flows*, Moss JN, Scott CD (eds). AIAA: New York, 1986; 478–513.
21. Yoon KT, Moon SY, Garcia SA, Heard GW, Chung TJ. Flowfield-dependent mixed explicit-implicit (FDMEI) methods for high and low speed and compressible and incompressible flows. *Computer Methods in Applied Mechanics and Engineering* 1998; **151**(1–2):141–219.
22. Hornung HG. Non-equilibrium dissociating nitrogen flow over spheres and circular cylinders. *Journal of Fluid Mechanics* 1972; **53**(1):149–176.

